1954-05

The Longitudinal Stability of the ZP2N-1 Airship

Layton, Donald M.; Iacobelli, Rocco F.

Princeton University

THE LONGITUDINAL STABILITY OF THE ZP2N-1 AIRSHIP

Donald M. Layton
and
Rocco F. Iacobelli

THE LONGITUDINAL STABILITY OF THE ZP2N-1 AIRSHIP

by

D. M. LAYTON
and
R. F. IACOBELLI

May 1954
Report No. 264

Princeton University
School of Engineering
Department of Aeronautical Engineering

Submitted in partial fulfillment of the requirements for the degree of Master of Science in Engineering from Princeton University, 1954.

ACKNOWLEDGMENTS

The writers of this report wish to express their appreciation to CAPT Ben May, USN, Commander of Naval Airship Training and Experimentation, who granted authorization to the writers to make flights in the ZP2N-1 airship. Further acknowledgment is made to CDR M. H. Eppes, USN and LCDR B. Levitt, USN, Senior Member and Secretary respectively of the Sub-Board of Inspection and Survey, U. S. Naval Air Station, Lakehurst, N. J. Through their cooperation flights in the airship were made available during acceptance trials. The assistance of LCDR Levitt and LCDR F. G. Carlstad, USN, in searching the files of the Sub-Board of Inspection and Survey was invaluable in the preparation of this report.

SUMMARY

A series of steady flight tests were made to determine the static longitudinal stability parameters of a U. S. Navy ZP2N-1 airship, and the results were compared with those computed from other considerations.

It was found that the steady state flight test values agreed with the computed values. The major differences encountered were due to basic inaccuracies in the test procedure. It was found that the airship was slightly unstable at low angles of attack. The stability at high angles of attack is attributed to the weight-buoyancy force.

TABLE OF CONTENTS

THE LONGITUDINAL STABILITY OF THE ZP2N-1 AIRSHIP

INTRODUCTION

Non-rigid airships have been flown satisfactorily in various sizes and configurations by commercial and military activities for many years. During World War II and following, there has been a military airship program of no small stature by the U. S. Navy. Although there was some in-flight investigation of the longitudinal stability of rigid airships in the 1920's, as far as is known, there have been no attempts to quantitatively investigate the longitudinal stability of the non-rigid type from flight data.

Subsequent to the late 1930's there has been a dearth of published information concerning the stability of lighter-than-aircraft. Inasmuch as there is no aerodynamic difference between a rigid airship and a similar non-rigid except for the minor considerations of skin drag due to differences in outer fabric, the theories developed for rigid airships hold well for non-rigids. Munk has established a reliable formula for the pitching

moment of a body of revolution; however, there has been no suitable method of theoretically or empirically determining the lift force generated by a body of revolution. Further, present means, both theoretical and empirical, do not accurately apply to the stabilizing surfaces because of the extremely low aspect ratio.

It was, therefore, proposed that this thesis should cover a modest attempt to investigate the static longitudinal stability of a U.S. Navy ZP2N-1 airship in flight with an aim to evaluate C_{L_α}, $C_{m_{\delta_e}}$, and C_{m_α}; to reconcile theory and practice; and to learn advantageous operating procedure.

Donald M. Layton

Rocco F. Iacobelli

PART I

SOURCES OF FORCES AND MOMENTS

AERODYNAMIC ENVELOPE MOMENT

The resulting pressure distribution on a body of revolution moving in a fluid at an angle of attack gives rise to a sizable pitching moment. Dr. Max Munk in his classic paper, Ref. 3, developed the equation for this aerodynamic moment of a body of revolution at an angle of attack.

$$M = \text{Volume} \times q \times (K_2 - K_1) \sin 2\alpha$$

where $(K_2 - K_1)$ is a factor relating the apparent mass of the air surrounding a cylinder to that of the apparent mass of the air surrounding an ellipsoid. $(K_2 - K_1)$ is a function of fineness ratio.

This aerodynamic moment taken at the center of volume is destabilizing in nature. Fig. 3 is a plot of C_m versus α for a bare airship hull and demonstrates this instability.

ENVELOPE LIFT AND RESULTING MOMENT EFFECT

A body of revolution in a perfect fluid experiences no lift with angle of attack. However, in a real fluid, an ellipsoid-type body of revolution developes vortices over the aft portion due to the separation of the flow. This vortex effect produces a lifting force acting at the rear of the body (Ref.4). Compared with an airfoil where the lifting force acts at the center of pressure

forward of the center of gravity thus creating an un-Stable moment, the lifting force on the bare hull of the airship generates a stabilizing moment (Fig. 3).

The lift developed by the envelope is of the order of one percent of the lift of an airfoil of equal surface area (Fig. 4). The value of this lift is a non-linear function of angle of attack and must be determined from wind tunnel tests (Ref. 5).

LIFT DUE TO STABILIZERS AND RESULTING MOMENT

Fins and control surfaces are attached to an airship hull to increase the dynamic stability and to provide for longitudinal and directional control. The conventional location of these surfaces is on the after part of the hull. These fins are of necessity large in order to counteract the aerodynamic pitching moment. Because of their size, a relatively large lift force is produced. Usually symetrical airfoil sections are used.

Due to the fact that the aspect ratio of the fins as conventionally computed is so small, the fins act more like wing tips than wing sections. An approximation to the variation of fin lift with angle of attack can be made from the equation:

$$L = \frac{2\pi q \alpha}{1 + \frac{S}{b^2}}$$

where S is the area of the fins plus the projection of

the envelope between the fins, and b is the span of the fin-envelope combination (Ref. 2).

Fin lift may be assumed to act at the quarter-chord of the fin. This, then contributes a stabilizing moment to the airship equal to the product of this lift and its lever arm.

For purposes of control, this stabilizer lift is augmented by elevator deflection (Fig. 5). The change in lift per degree of control deflection is a function of the ratio of elevator area to total stabilizer area.

DRAG AND DRAG MOMENT

The drag of an airship can best be determined from wind tunnel tests (Fig. 6), but can also be determined in level unaccelerated flight tests by equating thrust to drag. This assumes an accurate evaluation of thrust.

Since the profile and skin drag compose the major portion of the drag force, and since these two components are a function principally of the envelope, the drag force can be assumed to act near the center-line of the envelope.

Inasmuch as the drag equals the thrust, the moment due to drag can be incorporated in a couple due to drag and thrust. This couple will approximately equal the thrust multiplied by its distance to the envelope center-line.

THRUST AND THRUST MOMENT

Due to the form of the airship the engines are located below the envelope. Since the center of gravity usually falls about midway between the envelope centerline and the thrust line, the propellers produce a destabilizing moment.

As previously discussed, the combined moment of thrust and drag may be considered constant for a given level unaccelerated flight condition.

WEIGHT AND BUOYANCY FORCE AND MOMENT

A change in ballonet fullness can be considered as a shift of the lifting gas volume with a resultant shift in the center of buoyancy. The result is a change in the relative positions of the center of buoyancy and center of gravity. This is probably the most important consideration in the longitudinal stability of an airship in that it overcomes the inherent destabilizing aerodynamic moment at high angles of attack.

Since the weight or buoyant force moment is a function only of angle of attack, it can be reduced to coefficient form only for a particular velocity-angle of attack combination.

PART II

FLIGHT TEST ANALYSIS

DESCRIPTION OF THE AIRSHIP

This investigation was conducted in a U. S. Navy ZP2N-1 airship (Bureau number 126716). This airship which is sketched in Fig. 1 is the non-rigid type and has an overall length of 342.65 feet, an overall height of 96.77 feet, a maximum diameter of 75.42 feet, and a fineness ratio of 4.5. The empty gross weight is 46,302 pounds, and the maximum gross weight is 64,636 pounds. A static lift of 58, 636 pounds is derived from the buoyant force of helium at 0.062 pounds per cubic foot of lifting power when the envelope is 97 percent full. The design volume is 975,000 cubic feet.

The shape of the envelope is maintained by superpressure of the lifting gas. This superpressure (usually about 1.5 to 2.0 inches of water above atmospheric pressure) is produced by four variable volume air chambers (ballonets) within the envelope. Two ballonets are located side by side in the lower central portion of the envelope. The other two are in the lower forward and after sections of the envelope. The latter two ballonets serve an additional purpose of providing static trim. The effect of these ballonets, although each is only about five percent of the total volume, is considerable. A twenty percent change in volume of the fore and aft ballonets can make as much as a

fifteen foot difference in the position of the center of buoyancy.

The airship is powered by two Wright R-1300-2 engines mounted in the car. These with normal shafting arrangement drive two Curtis 16.7 foot adjustable pitch propellers. The shafting and clutch arrangements are such as to provide two-engine two-propeller, single-engine single-propeller, or single-engine two-propeller operation. The thrust axis of the propellers is 46.3 feet below the center-line of the envelope.

The most unusual part of the aerodynamic configuration is the stabilizing and control surfaces. The four surfaces are mounted 45 degrees to the vertical and horizontial. Because of this arrangement the control surfaces are called ruddevators. The total surface has its aerodynamic center located 290 feet aft of the theoretical bow. Such an arrangement has the twofold advantage of presenting more ground clearance under the tail surfaces and of furnishing more effective surface components in the horizontal and vertical planes.

Pilot control is obtained from a yoke type control. Fore and aft movement and wheel movement of the yoke are mechanically fed into a mixing box and hydraulic boost which gives a combination of ruddervator angles providing the longitudinal and directional control desired.

INSTRUMENTATION

The instrumentation used to record the flight test data was incorporated in the photo-observer panel. This panel, shown in Fig. 2, was located in the CIC compartment of the airship. This panel consisted of an illuminated instrument panel with a 35 mm motion picture camera. This equipment was installed by the Goodyear Aircraft corporation for the use in contractor flight tests and for use by the U. S Navy BIS trials.

The ruddevator position indicators consisted of 24 volt DC selsyn type transmitters geared to a rigid fin linkage and selsyn type indicors on the photo panel. Each indicator presented indication of the deflection of one control surface.

The pitch attitude of the airship was obtained from a modified Norden Type C-1 vertical displacement gyro. The output of the gyro was directed through a balancing unit to a Weston 301 milliameter. The milliameter dial was adapted to read from minus one to plus one with graduated divisions.

The airspeed indicator, Kollsman 586 BK-1-0153, was modified to provide dial increments of one knot. The airspeed-pitot static system consisted of two Kollsman 5816-2 (Round head without shark fin) pitot heads, with fixes, installed on a boom extending forward and

on the center-line below the car level. The boom was tilted up 12 degrees to be in the airstream about the envelope.

The altimeter, Kollsman KN 05, obtained pressure from the airspeed system.

The outside air temperature installation was powered from the photo-observer switch unit and the bulb was located on the starboard side above the utility compartment door.

The run number was displayed on the photo-observer panel by means of a mechanical counter. The counter was operated by a soleniod which was energized by the camera switch on the switch box.

All dials were initially manually positioned to zero and calibrated throughout the range. Flight calibration was made by voltage-deflection adjustment of the balance box.

The airspeed system installation was initially calibrated by the use of an NACA trailing static head. In-flight verification was made by comparison to a similar head.

FLIGHT TEST PROCEDURE

All flight tests were conducted at the U. S. Naval Air Station, Lakehurst, N. J. Test data was recorded during regularly scheduled flights of the Navy Sub-Board of Inspection and Survey Trials on a non-interference basis. This requirement limited the scope of the investigation, but in no way hindered the conduct of the tests.

Test data was obtained from four series of runs at static heavinesses of 3,000, 3,750, 5,000, and 6,000 pounds made at constant altitude. In each run series, airspeed was varied from approximately 35 knots to 60 knots in about five knot increments. The following data was recorded:

Outside air temperature
Pressure altitude
Airspeed
Angle of pitch = angle of attack in level flight
Ruddevator angles
Static heaviness
Center of gravity location
Center of buoyancy location
Gross weight

The center of buoyancy was maintained constant throughout each run series. The propeller pitch was maintained constant at 16.5 degrees during the speed changes, because this was the only propeller setting

for which the manufacturer had provided brake horsepower versus velocity data.

Pre-flight tests included the obtaining of weight and balance data and the static heaviness. The former determined the location of the center of gravity and the center of buoyancy and the latter envolved the calculation of the difference between the gross weight and buoyant force. A calibration of the photo-observer panel was also made as part of the pre-flight operation.

Constant weight and balance control was maintained by fuel, fuel flow, and water ballast readings. The fullness of the ballonets was periodically measured by visual inspection in order to ascertain the location of the center of buoyancy.

FLIGHT TEST DATA REDUCTION

The flight test data was reduced by normal data reduction methods. V_m was converted to V_{cal} from a calibration curve provided with the instrumentation. Temperature and pressure altitude were used to enter a density and pressure altitude conversion chart to obtain density ratio. From this dynamic pressure was computed.

Then:
$$C_L = \frac{\text{Static Heaviness}}{qV^{2/3}}$$

Angle of attack was considered to be equal to the angle of pitch in level flight. The milliameter reading was converted to pitch angle by multiplying by the

factor 30.6.

$$\alpha = \text{ma.} \times 30.6$$

Ruddervator deflection was converted from the voltmeter reading by multiplying by the factor, 0.333.

$$\delta_e = \text{volts} \times 0.333$$

The equivalent elevator deflection then equals the algebraic sum of all ruddevator deflections divided by four.

Thrust was determined by converting brake horsepower obtained from curves provided by the manufacturer. Since no propeller curves were available covering the low velocities at which an airship operates, a constant efficiency of eighty percent was assumed.

$$T = \frac{BHP}{V} \times 0.8$$

PRESENTATION OF DATA

In order to present the data in a more manageable form, all forces and moments have been reduced to coefficient form. The forces are computed utilizing characteristic area of volume to the two-thirds power, and the moments using the characteristic dimension of volume. In order to convert forces to moments, a non-dimensional distance of lever arm divided by volume to the one-third is employed. All moments will be referred to the center of buoyancy.

For the presentation of meaningful airship flight test data it is necessary to conduct runs under two conditions. The first condition is to obtain C_L versus α, holding center of gravity location and elevator deflection constant while varying the center of buoyancy location with airspeed. The second condition is to obtain C_L versus α (C_L required to trim), holding center of gravity and buoyancy locations constant while elevator is changed with airspeed.

This gives a series of C_L versus curves at various δ_e with a superimposed plot of C_L required to trim for given center of gravity and center of buoyancy locations (Fig. 9).

The derivative C_{L_α} is obtained directly from the plots by measuring the slope of the C_L versus curves. $C_{m_{\delta_e}}$ is then readily obtained by considering the change in C_L at a constant α due to elevator deflection. Then

$$C_{m_{\delta_e}} = \frac{C_L}{\delta_e} \frac{l_t}{V^{1/3}}$$

This is slightly in error in that the change in lever arm of the tail between the points is not considered.

The plot of C_m versus α for a given δ_e and center of gravity and center of buoyancy location is obtained by use of the C_L required to trim curve. This is done in the following manner. Consider an α given by the intersection of C_L to trim an a C_L versus α at some δ_e curves. This gives a trim point i.e. $C_m = 0$. Now by

taking other points at the same α on other C_L versus α curves values of C_m for other δ_e are determined by multiplying the change in C_L by the non-dimensional lever arm of the tail. If this same procedure is followed at other trim points a series of moment coefficients for each elevator angle is obtained and plots of C_m versus α are made (Figs. 7 and 8). Again this is slightly in error because the tail lever arm was considered constant when it actually varied by a few percent.

It was not practicable to change the center of buoyancy in order to maintain a constant elevator angle through each series of runs, therefore, it was decided to fit the flight test data to data reduced from wind tunnel test of a similar model.

The wind tunnel data (obtained from Ref. 5) was corrected for thrust and weight moments. Since moments are considered about the center of buoyancy, which is very close to the center-line of the envelope, the correction for thrust moment was thrust multiplied by its distance to the center-line. Drag was considered to act at the center of buoyancy.

The weight moment arm is a function of angle of attack since the center of gravity is located about 29 feet below the center of buoyancy. The angle of zero weight moment was determined from a static trim check.

$$M_w = \text{(gross weight)}\ 29\sin(\alpha_{st} - \alpha)$$

The tail configuration of the wind tunnel model was that of vertical and horizontal stabilizers. It was therefore necessary to correct the elevator deflection by a factor of $\sqrt{2}$. In addition, a correction was made due to the difference in the $\frac{S_e}{S_t}$ ratios. These were the only corrections considered necessary because the ratio $\frac{S_t}{V^{2/3}}$ of the model and the test vehicle are about the same.

After applying these corrections to the wind tunnel data new plots of C_L versus α and C_L required to trim and C_m versus α corresponding to the 3,000 pound heavy run were made.

Data from all runs is superimposed on the C_L versus α curves. Here, for $\delta_e = 1^o$, values of $1^o \pm 0.3^o$ were used. The same policy was used for $\delta_e = 2^o$ and 3^o. Only the data from the 3,000 pound heavy run is used to compare C_L required trim with that computed.

DISCUSSION AND RESULTS

The comparison of the flight test data with that reduced from wind tunnel tests does show some correlation in that the stability deratives may be assumed to fall in the same neighborhood of those derived from the wind tunnel test results. It will be noted, however, from the plot of test points some searching of the

imagination would be required to determine any thing from the test results if there had been nothing with which to compare them.

The wide scatter of points can be attributed to the fact that it was attempted to secure steady flight information at unstable points. Such an undertaking is not considered impossible, but in order to meet with any success it should be attempted only in the most still air. The test results incorporated in this report were not obtained under these ideal conditions.

It is demonstrated in Fig. 10 that decreasing the nose-up angle for trim decreases the lift coefficient required for trim at an angle of attack. Since these curves are plotted for a constant value of dynamic lift, a decrease in lift coefficient with angle of attack is equivalent to increasing velocity required to trim at a given angle of attack.

By increasing the nose-up angle of angle of trim (''trimming aft'') the airship may be flown in a dynamic trim (albeit unstable) at lower angles of attack. The expected loss of lift with decreased angle of attack is compensated by the lift resulting from the increase in down elevator.

The instability shown by Figs. 7 and 8 is neither unusual nor fatal. The dynamic instability is so slug-

gish that the static instability fails to be critical. It is to be noted that the instability is reduced by decreasing the nose-up angle of static trim.

Although it is not readily apparent from a qualitative appraisal of Fig. 6, it might be more easily seen from physical considerations that an airship at low angle of attack with down elevator will have less drag than an airship with neutral elevator at high angle of attack. This should be obvious from the considerations of profile drag alone.

This decrease in drag is equivalent to a decrease in thrust required. It is therefore possible to trim aft and by using down elevator for dynamic trim, fly at the same velocity with less power.

This has far reaching implications in operational usage. The possibility of flight at reduced power produces indications of increased range and increased endurance, and flight at reduced angle of attack which is advantageous for radar operation.

CONCLUSIONS AND RECOMMENDATIONS

The results in this report obtained from flight test are by themselves quantitatively inconclusive, but when compared with more closely controlled wind tunnel tests show some correlation. This correlation when applied to the evaluation of elevator power confirms the expect increase of $C_{m_{\delta_e}}$ due to the ruddervator arrangement.

The static instability at low angles of attack previously evaluated in qualitative flight tests was to a degree quantitatively confirmed.

From the evaluation of the effect of tail heaviness reducing angle of attack for C_L required to trim it can be concluded that this arrangement is benificial to fuel economy and advantageous when the airship is used as a radar platform. Further quantitative evaluation in this subject is recommenced.

The statement of Dr. Karl Arnstein in Ref. 2, "The experimental determination of the dynamic lift characteristics of the complete airship, full size, is a very delicate problem." is definitely confirmed. The results of this investigation though quantitatively inconclusive are not disheartning. Therefore it is recommended that such an investigation be undertaken again with an airship of unlimited availibility and the employment of a delicate touch.

References

1. Perkins, C. D. and Hage, R. E. Airplane Performance, Stability and Control, (John Wiley and Sons, 1950)

2. Durand, W. F. Aerodynamic Theory Volume VI; Division Q by Munk, M. M.; Division R by Arnstein, K. and Klemperer, W.

3. NACA Report 184 "The Aerodynamic Forces on Airship Hulls" by Munk, M. M.

4. NACA TN 106 "Notes on Aerodynamic Forces III" by Munk, M. M.

5. Daniel Guggenheim Airship Institute "Wind Tunnel Tests of an M-Type Airship Model" by Champney, W. B., Akron, Ohio, 1942

6. Frazer, R. A. and Bateman, H. "Measurement of Normal Force and Pitching Moment of Rigid Airship R 33" Br. A.R.C. R. and M. 815, 1922

TABLE I

Test Results, Run Series N°. 1

Run N°.	V_m Knots	m.a. Pitch	Volts-Ruddevator Deflection			
			Upper Port	Lower Port	Upper Stbd	Lower Stbd
1	59.0	0.05	-15	10	5	-20
2	60.0	0.02	-9	-5	-5	-7
3	56.0	0.09	-12	-12	-11	-11
4	54.5	0.13	-9	-9	-14	-5
5	49.5	0.05	-8	-5	-6	-7
6	50.5	0.06	-10	-11	-16	-5
7	47.5	0.09	-3	-14	-20	-4
8	45.5	0.12	-12	-6	-10	-10
9	40.0	0.18	——	——	——	——
10	41.5	0.11	-11	-11	-17	-5
11	35.5	0.18	-12	-6	-8	-10
12	35.5	0.24	-12	-11	-14	-15

Temperature: -5°C

Pressure Altitude: 1000 feet

Static Heaviness: 6000 lbs.

TABLE II

Test Results, Run Series No. 2

Run No.	V_m Knots	m.a. Pitch	Volts-Ruddevator Deflection			
			Upper Port	Lower Port	Upper Stbd	Lower Stbd
14	58.0	0.03	3	-5	-5	-1
15	57.5	0.02	-2	1	6	-6
16	55.0	0.02	0	0	-4	-1
17	54.5	0.01	0	0	-3	-5
18	50.0	0.04	0	-3	-3	-3
19	50.0	0.06	-2	-1	0	-6
20	43.5	0.09	3	-2	-4	-3
21	44.0	0.06	2	-1	-3	-1
22	38.0	0.12	4	-2	-2	0
23	39.0	0.05	2	-2	-2	-2
24	36.1	0.11	2	-6	-1	-14
25	36.4	0.05	2	0	1	-2
26	35.5	0.11	-2	-1	0	-6
27	30.0	0.06	-7	-6	-9	-7
28	30.5	0.06	-8	-6	-6	-7

Temperature: -3°C

Pressure Altitude: 1000 feet

Static Heaviness: 3000 lbs.

TABLE III

Test Results, Run Series N°. 3

Run N°.	V Knots	m.a. Pitch	Volts-Ruddevator Deflection			
			Upper Port	Lower Port	Upper Stbd	Lower Stbd
1	32.2	0.29	2	-2	-3	12
2	38.0	0.25	-3	-2	-1	-4
3	42.0	0.21	-7	-2	-5	-5
4	51.0	0.11	-5	-2	-6	-5
5	50.0	0.06	-4	-6	-11	-4
6	50.5	0.09	-7	-2	-6	-7
7	53.0	0.12	-9	-8	-11	-8
8	55.0	0.08	-2	-7	-11	-4
9	54.0	0.02	-3	-1	2	-4
10	55.0	0.10	-3	-3	-8	-2
11	59.0	0.06	-4	-6	-10	-5
12	60.0	0.02	-10	-2	-2	-8

Temperature: 0°C

Pressure Altitude: 1200 feet

Static Heaviness: 5000 lbs.

TABLE IV

Test Results, Run Series N°. 4

Run N°.	V_m Knots	m.a. Pitch	Volts-Ruddevator Deflection			
			Upper Port	Lower Port	Upper Stbd	Lower Stbd
20	33.0	0.10	-6	-8	-10	-8
21	31.0	0.25	4	1	1	3
22	39.0	0.18	2	1	2	0
23	38.0	0.18	6	-1	-2	2
24	44.0	0.09	-3	-2	-2	-6
25	45.0	0.11	2	-2	-4	0
26	51.0	0.02	-1	0	0	-4
27	52.0	0.11	-3	3	8	-7
28	53.0	0.08	0	-1	-2	-2
29	55.0	0.09	7	-10	-15	6
30	56.0	0.08	0	0	0	-2
31	56.0	0.10	-7	2	3	-10
32	58.0	0.07	3	-7	-12	-2
33	58.0	0.02	5	-4	-1	5
34	60.0	0.01	0	0	0	-2

Temperature: 4°C

Pressure Altitude: 1500 feet

Static Heaviness: 3750 lbs.

TABLE V

Reduced Results, Run Series No. 1

Run No.	V_{cal} Knots	α Degrees	δ_e Degrees	C_L
1	60.0	1.53	-1.67	0.0505
2	60.7	.61	-2.83	0.0493
3	57.0	2.75	-3.83	0.0585
4	55.5	3.98	-3.08	0.0585
5	51.0	1.53	-2.83	0.0682
6	52.0	1.84	-3.50	0.0656
7	49.0	2.75	-3.42	0.0745
8	47.0	3.68	-3.50	0.0809
9	41.3	5.51	-	0.1052
10	42.7	3.37	-3.67	0.1000
11	36.6	5.51	-3.00	0.1342
12	36.6	7.35	-4.33	0.1342

TABLE VI

Reduced Results, Run Series N°. 2

Run N°.	V_{cal} Knots	α Degrees	δ_e Degrees	C_L
14	58.0	0.92	-0.67	0.0252
15	57.5	0.61	-0.08	0.0262
16	55.0	0.61	-0.33	0.0281
17	54.5	0.31	-0.67	0.0284
18	50.0	1.22	-0.75	0.0329
19	50.0	1.84	-0.75	0.0329
20	43.5	2.75	-0.30	0.0438
21	44.0	2.49	-0.25	0.0435
22	38.5	2.75	0	0.0556
23	39.0	1.84	-0.33	0.0542
24	36.1	3.68	-1.17	0.0647
25	36.4	1.53	0.08	0.0620
26	35.5	3.37	0.75	0.0655
27	30.0	1.53	-2.42	0.0888
28	20.5	1.84	-2.23	0.0868

TABLE VII

Reduced Results, Run Series N°. 3

Run N°.	V_{cal} Knots	α Degrees	δ_e Degrees	C_L
1	33.3	8.80	-0.75	0.1311
2	39.4	7.65	-0.83	0.0964
3	43.1	6.42	-1.58	0.0809
4	52.5	3.36	-1.83	0.0533
5	51.4	1.84	-2.08	0.0550
6	52.0	2.75	-1.83	0.0537
7	54.2	3.67	-3.00	0.0500
8	56.0	2.45	-2.67	0.0476
9	55.0	0.61	-0.30	0.0490
10	56.0	3.06	-1.33	0.0476
11	59.8	1.84	-2.08	0.0419
12	60.7	0.61	-1.83	0.0405

TABLE VIII

Reduced Results, Run Series N°. 4

Run N°.	V_{cal} Knots	α Degrees	δ_e Degrees	C_L
20	34.0	3.06	-2.67	0.0920
21	32.0	7.65	-0.75	0.1089
22	40.2	5.51	0.42	0.0709
23	39.3	5.51	0.42	0.0747
24	46.2	2.75	-1.08	0.0562
25	46.2	3.36	-0.33	0.0334
26	52.4	0.61	-0.42	0.0472
27	51.5	3.36	0.08	0.0426
28	53.5	2.45	-0.42	0.0399
29	54.2	2.75	-1.33	0.0386
30	56.0	2.45	-0.17	0.0366
31	57.0	3.06	-1.00	0.0352
32	57.0	2.14	-1.83	0.0328
33	57.0	0.61	-0.42	0.0328
34	60.7	0.31	-0.17	0.0312

ZP2N-1 AIRSHIP

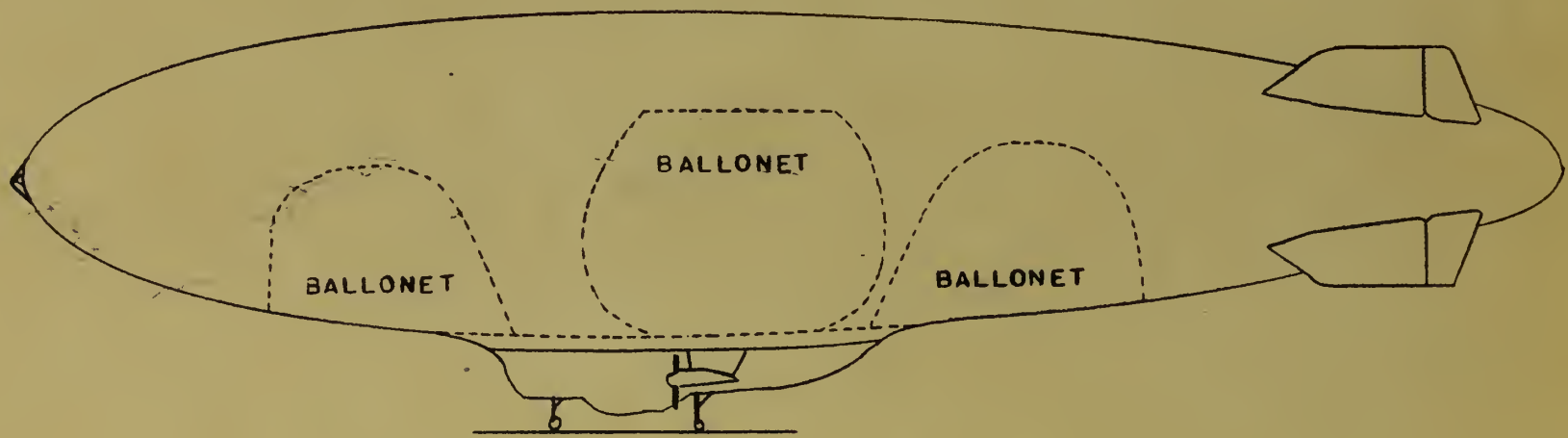

FIGURE 1

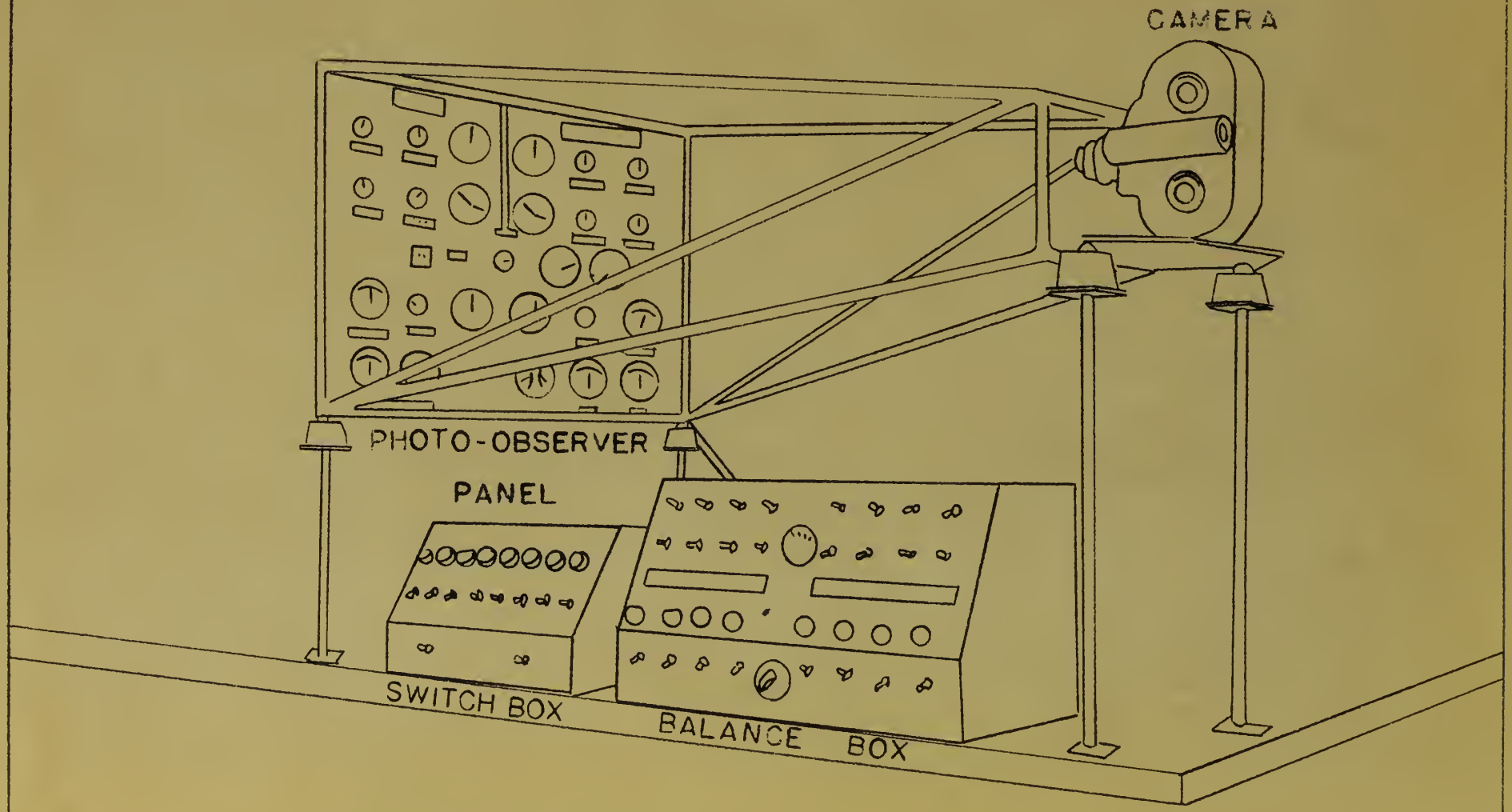

INSTRUMENTATION

FIGURE 2

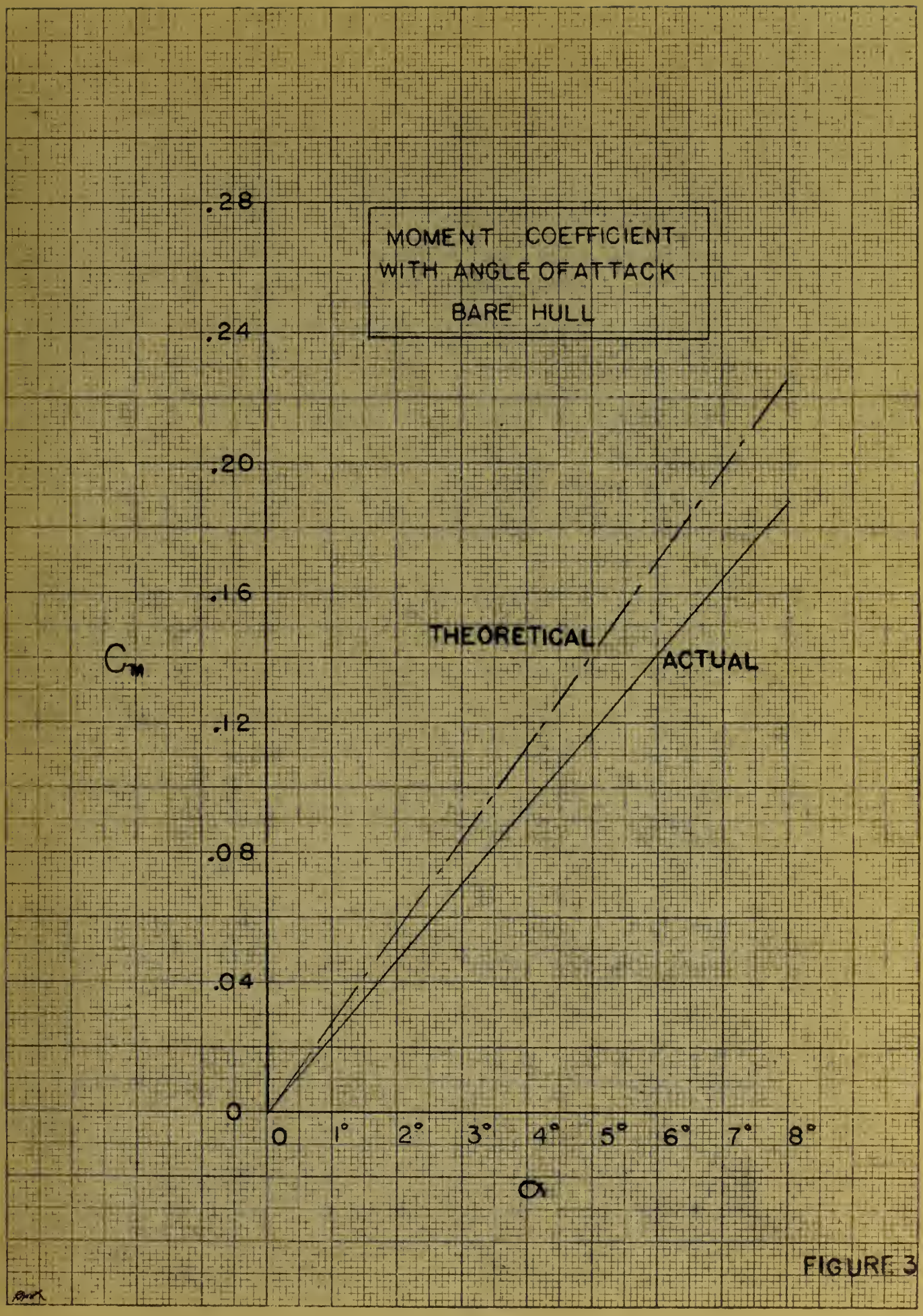
MOMENT COEFFICIENT
WITH ANGLE OF ATTACK
BARE HULL
.28
.24
.20
.16
.12
.08
.04
0
C_m
THEORETICAL
ACTUAL
0
1°
2°
3°
4°
5°
6°
7°
8°
α

FIGURE 3

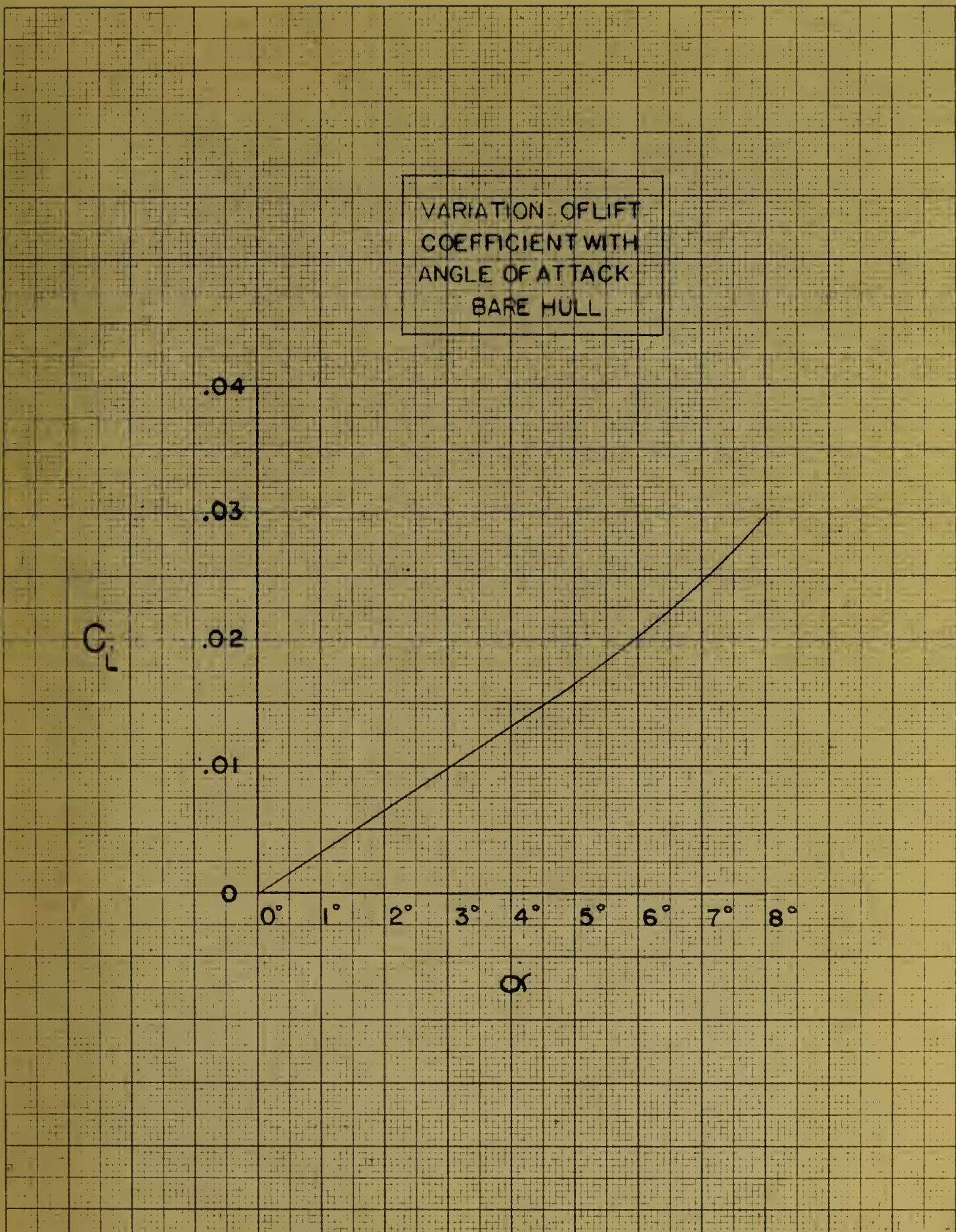
VARIATION OF LIFT COEFFICIENT WITH ANGLE OF ATTACK BARE HULL
.04
.03
.02
.01
0
C_L
0°
1°
2°
3°
4°
5°
6°
7°
8°
α

FIGURE 4

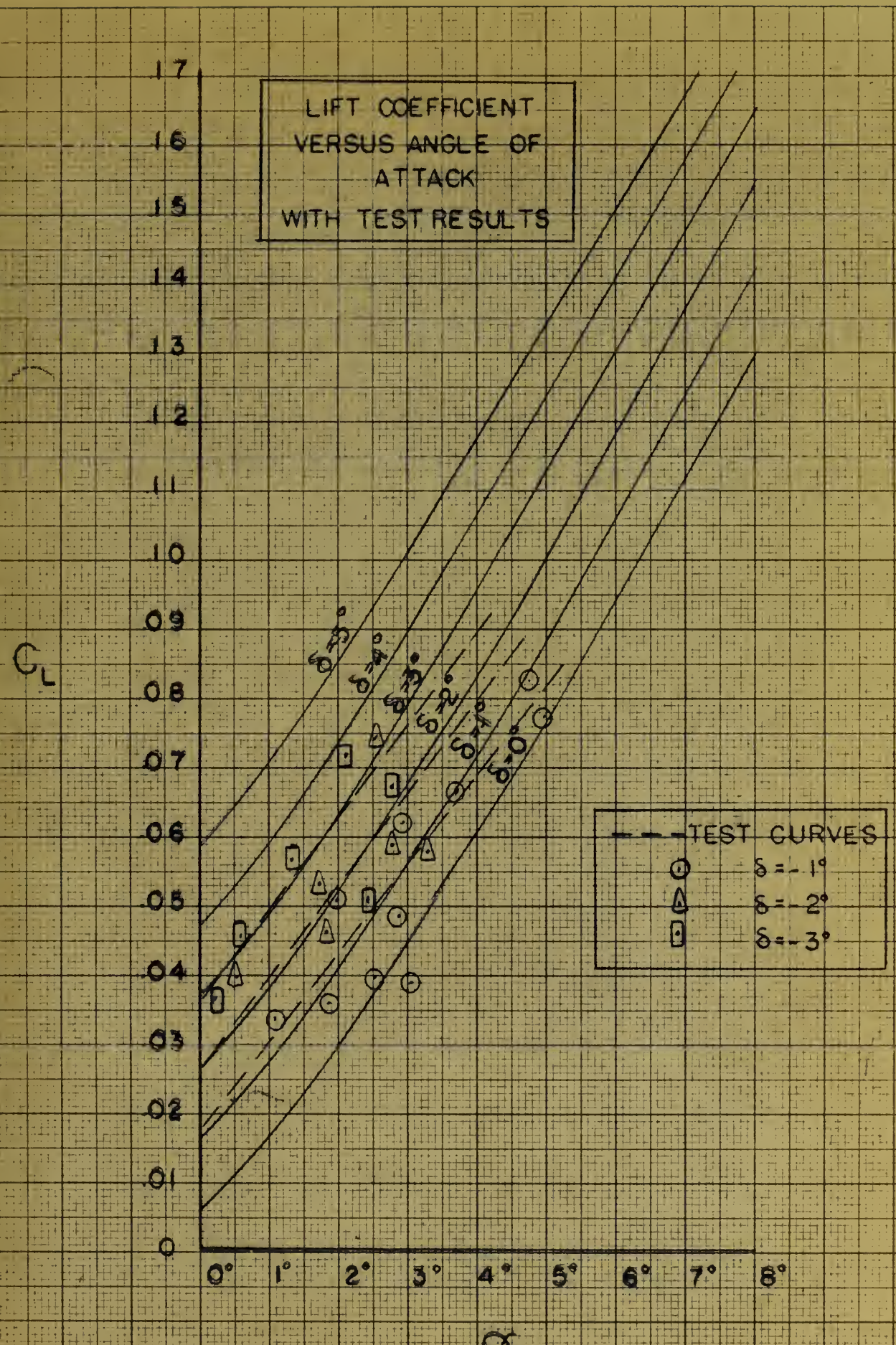
LIFT COEFFICIENT VERSUS ANGLE OF ATTACK WITH TEST RESULTS
C_L
1.7
1.6
1.5
1.4
1.3
1.2
1.1
1.0
.9
.8
.7
.6
.5
.4
.3
.2
.1
0
0°
1°
2°
3°
4°
5°
6°
7°
8°
α
TEST CURVES
δ = -1°
δ = -2°
δ = -3°

FIGURE 5

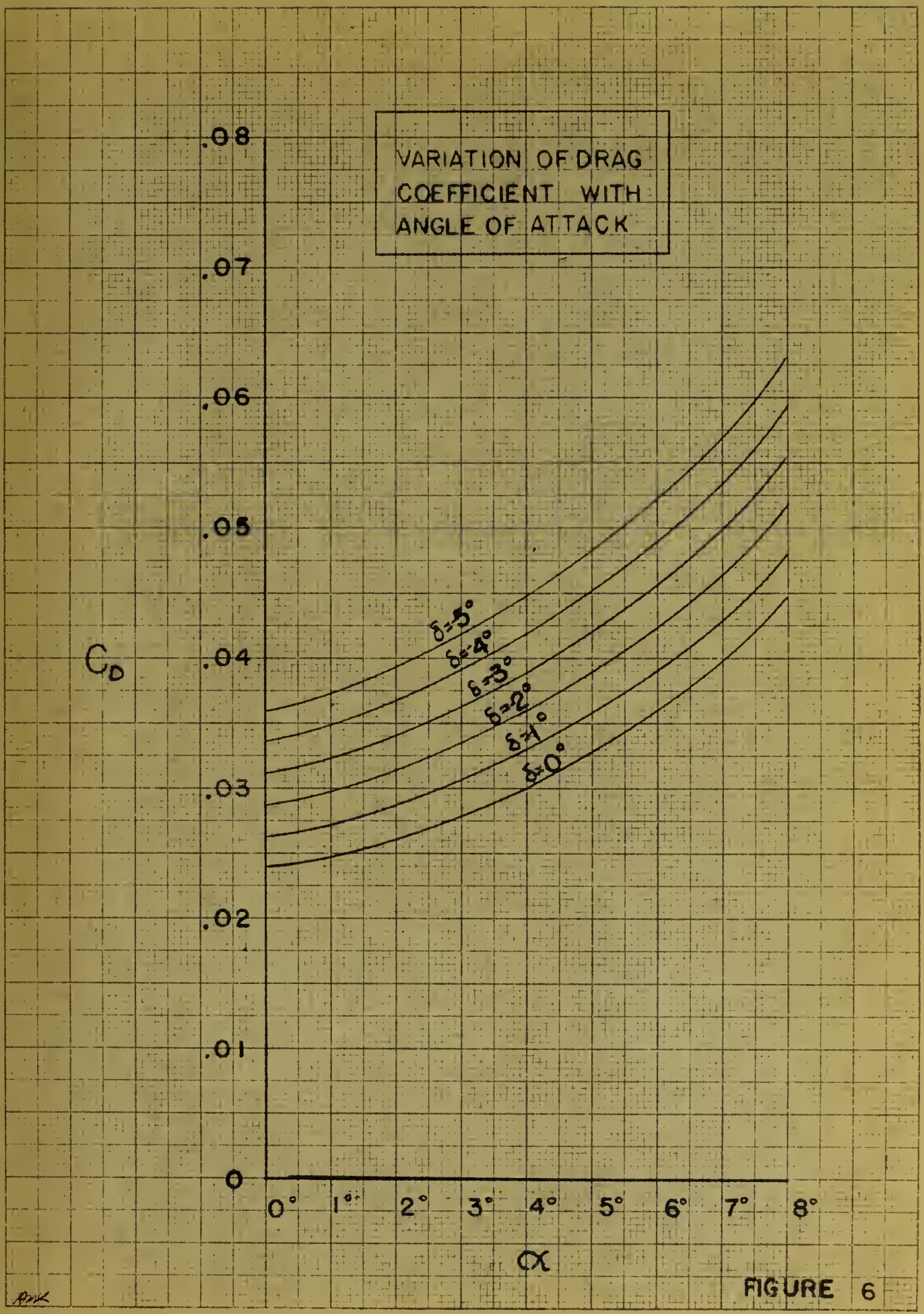
VARIATION OF DRAG COEFFICIENT WITH ANGLE OF ATTACK
.08
.07
.06
.05
.04
.03
.02
.01
0
C_D
δ=5°
δ=4°
δ=3°
δ=2°
δ=1°
δ=0°
0°
1°
2°
3°
4°
5°
6°
7°
8°
α

FIGURE 6

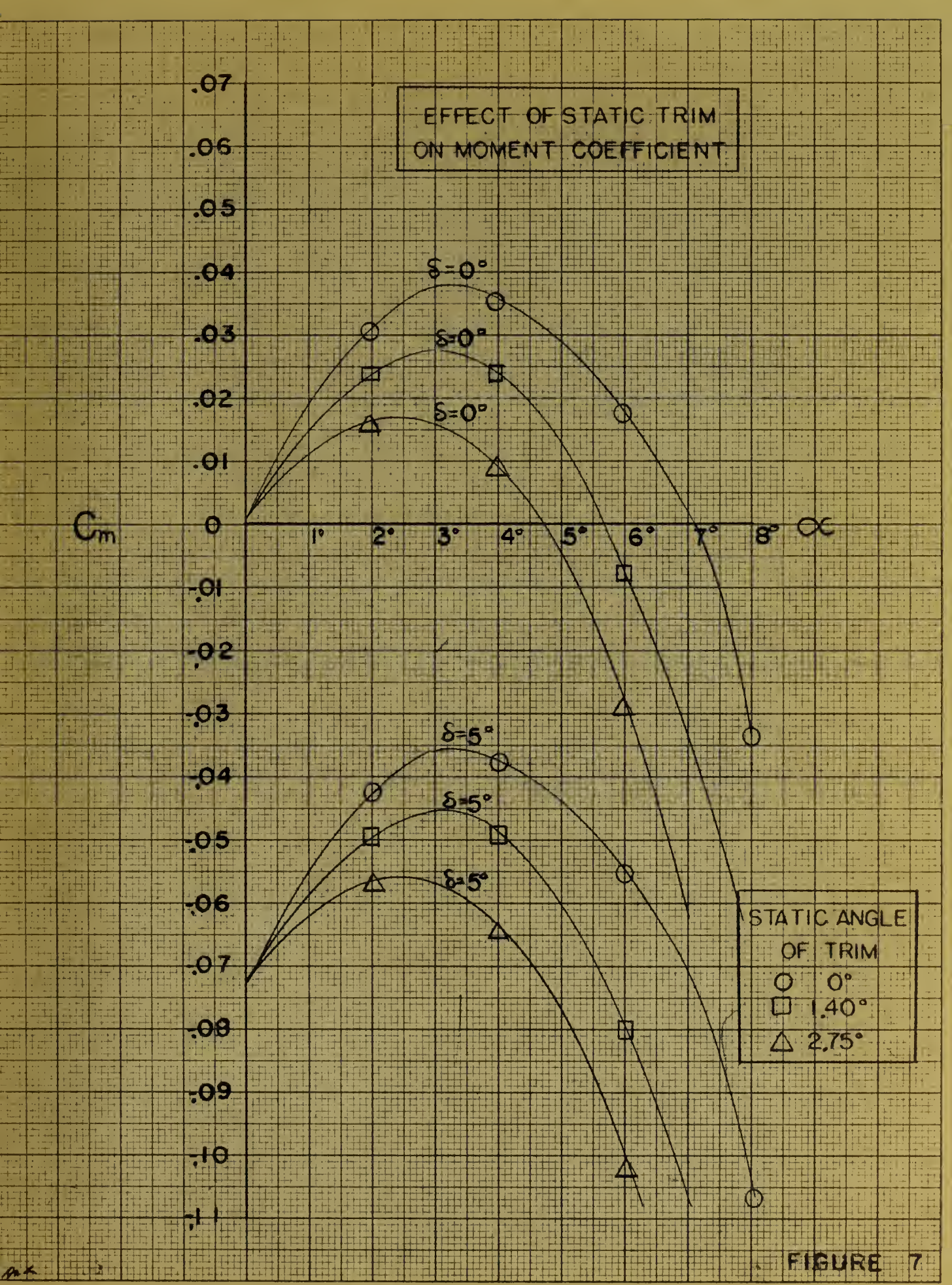
EFFECT OF STATIC TRIM
ON MOMENT COEFFICIENT
.07
.06
.05
.04
.03
.02
.01
0
-.01
-.02
-.03
-.04
-.05
-.06
-.07
-.08
-.09
-.10
-.11
Cm
1°
2°
3°
4°
5°
6°
7°
8°
α
δ=0°
δ=0°
δ=0°
δ=5°
δ=5°
δ=5°
STATIC ANGLE
OF TRIM
0°
1.40°
2.75°

FIGURE 7

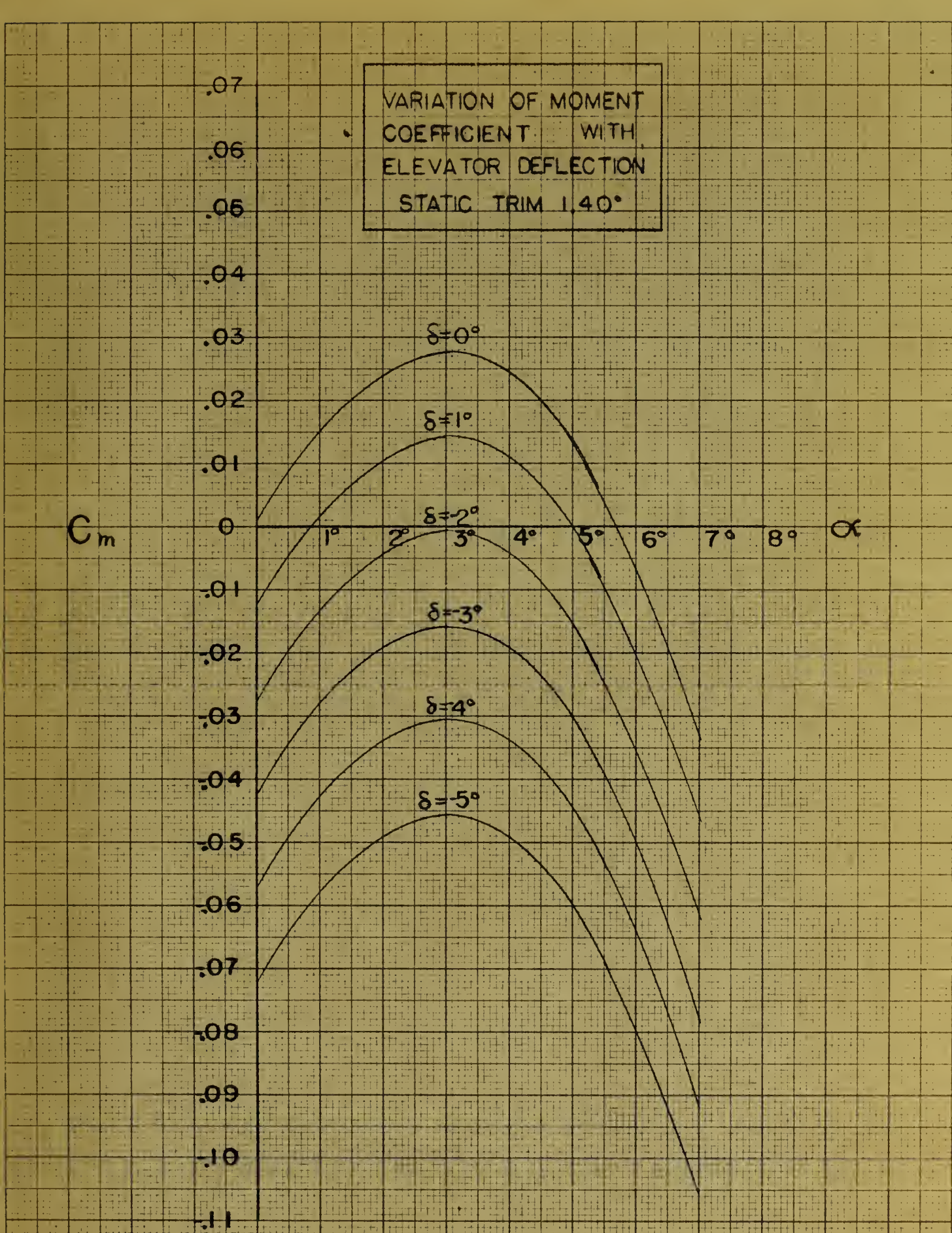
VARIATION OF MOMENT COEFFICIENT WITH ELEVATOR DEFLECTION
STATIC TRIM 1.40°
.07
.06
.05
.04
.03
.02
.01
0
-.01
-.02
-.03
-.04
-.05
-.06
-.07
-.08
-.09
-.10
-.11
C_m
1°
2°
3°
4°
5°
6°
7°
8°
α
δ=0°
δ=1°
δ=-2°
δ=-3°
δ=-4°
δ=-5°

FIGURE 8

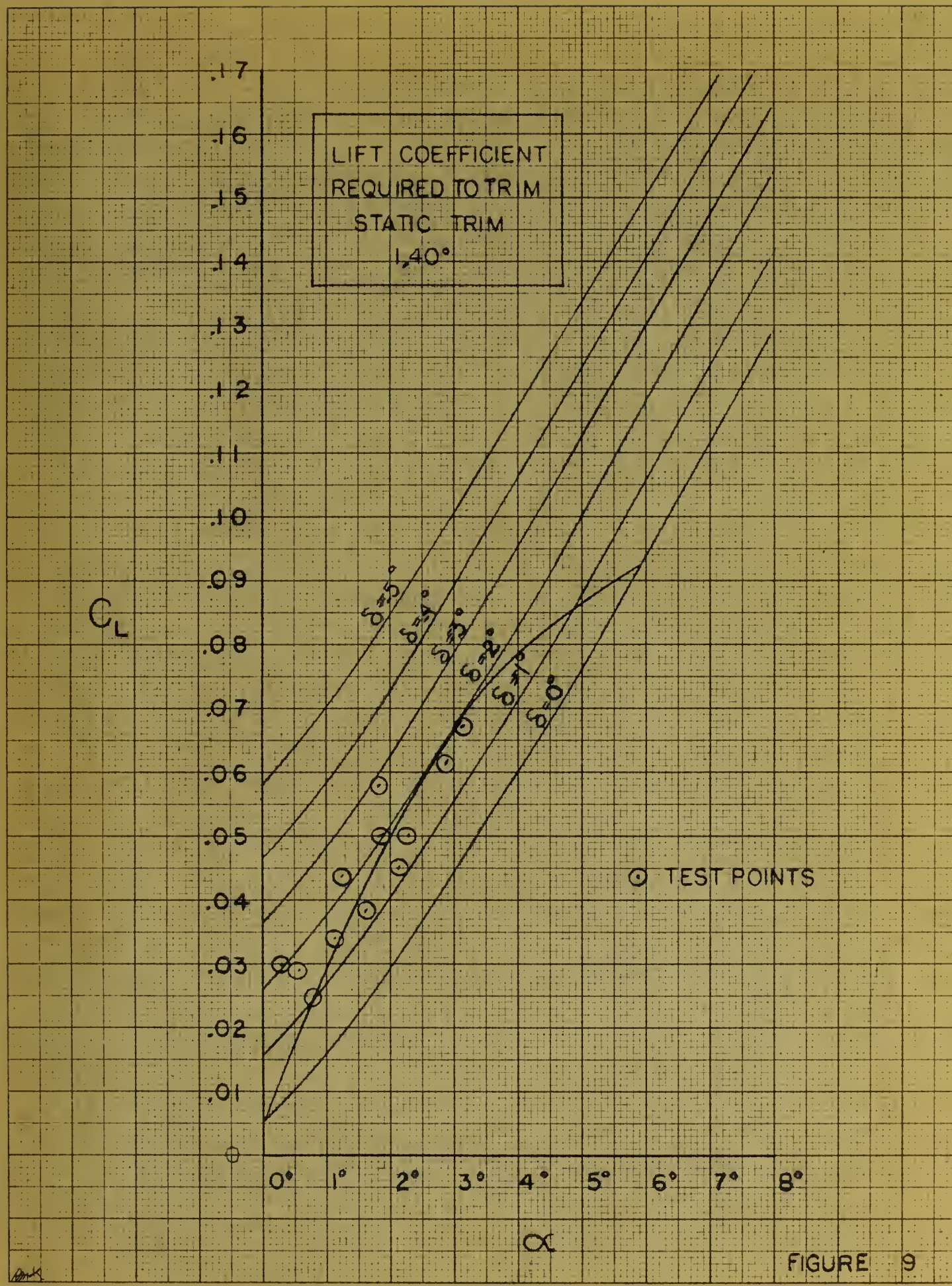
LIFT COEFFICIENT
REQUIRED TO TRIM
STATIC TRIM
1.40°
C_L
.17
.16
.15
.14
.13
.12
.11
.10
.09
.08
.07
.06
.05
.04
.03
.02
.01
0
0°
1°
2°
3°
4°
5°
6°
7°
8°
α
$\delta_f = 50°$
$\delta_f = 40°$
$\delta_f = 30°$
$\delta_f = 20°$
$\delta_f = 10°$
$\delta_f = 0°$
⊙ TEST POINTS

FIGURE 9

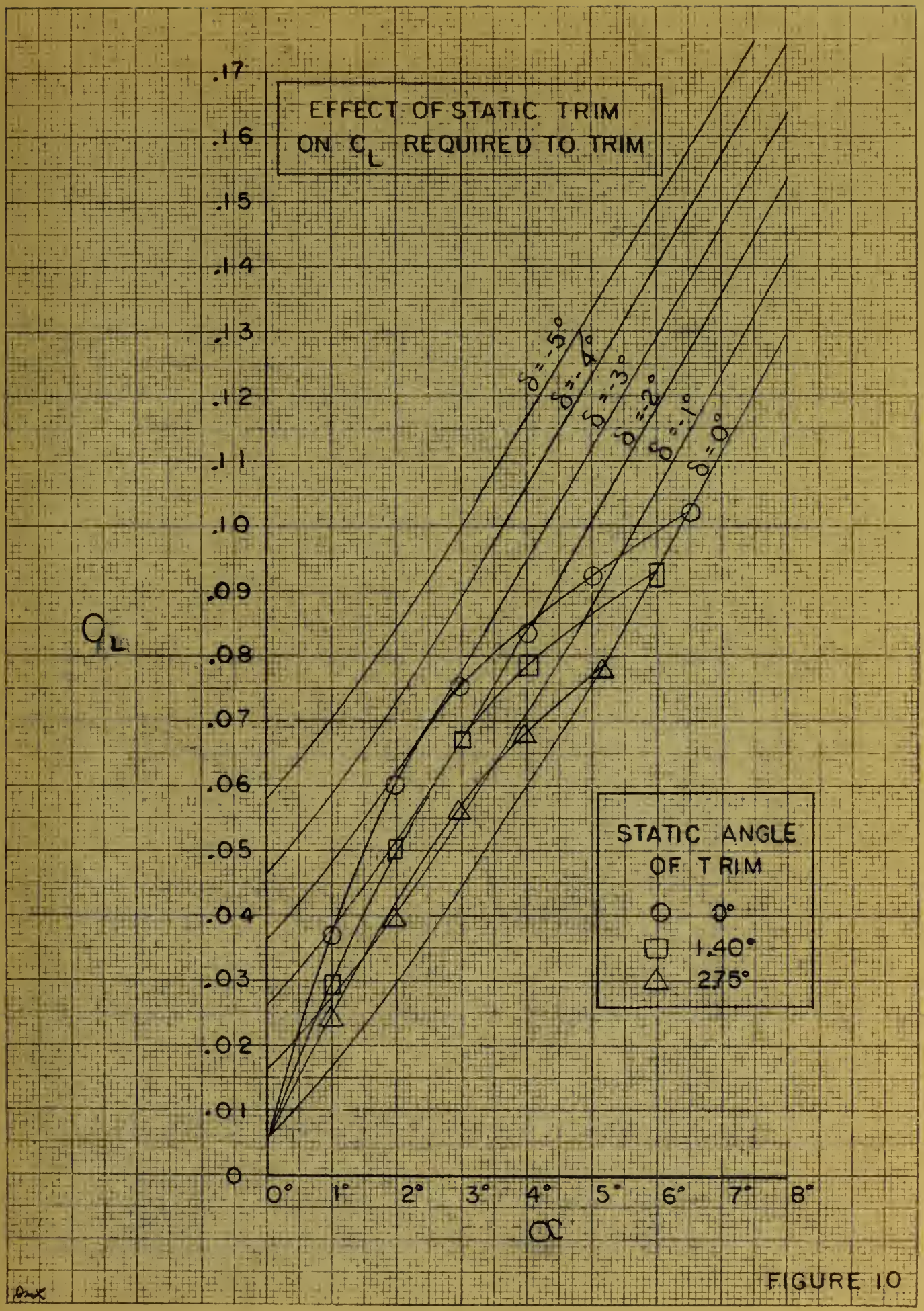
EFFECT OF STATIC TRIM ON C_L REQUIRED TO TRIM
C_L
.17
.16
.15
.14
.13
.12
.11
.10
.09
.08
.07
.06
.05
.04
.03
.02
.01
0
0°
1°
2°
3°
4°
5°
6°
7°
8°
α
$\delta = -5°$
$\delta = -4°$
$\delta = -3°$
$\delta = -2°$
$\delta = -1°$
$\delta = 0°$
STATIC ANGLE OF TRIM
0°
1.40°
2.75°

FIGURE 10